New Higher-resolution Discrete Euclidean Medial Axis in nD with Linear Time Parallel Algorithm

André Vital Saúde*
Federal University of Lavras, Department of Computer Science
CP 3037, 37200-000 Lavras/MG, Brazil
saude@ufla.br

Abstract

The notion of skeleton plays a major role in shape analysis since the introduction of the medial axis. The continuous medial axis is a skeleton with the following characteristics: centered, thin, homotopic, and reversible (sufficient for the reconstruction of the original object). The discrete Euclidean medial axis (MA) is also reversible and centered, but no longer homotopic nor thin. To preserve topology and reversibility, the MA is usually combined with homotopic thinning algorithms. Since there is a robust and well defined framework for fast homotopic thinning defined in the domain of abstract complexes, some authors have extended the MA to a doubled resolution grid and defined the discrete Euclidean Medial Axis in Higher Resolution (HMA), which can be combined to the framework defined on abstract complexes. Other authors gave an alternative definition of medial axis, which is a reversible subset of the MA, and is called Reduced Discrete Medial Axis (RDMA). The RDMA is thinner than the MA and can be computed in optimal time. In this paper we extend the RDMA to the doubled resolution grid and we define the High-resolution RDMA (HRDMA). The HRDMA is reversible and it can be computed in optimal time. The HRDMA can be combined with the algorithms in abstract complexes, so a reversible and homotopic Euclidean skeleton can be computed in optimal time.

Key Words: medial axis, skeleton, Euclidean distance, shape representation

1 Introduction

The notion of skeleton plays a major role in shape analysis since Blum introduced the concept of medial axis in 1967 [1]. The Euclidean medial axis is the set of centers of maximal Euclidean balls in the object, where a maximal ball is a ball contained in the object and not contained in any other ball in the object. The Euclidean medial axis of a continuous shape is a skeleton with the following characteristics: centered, thin, homotopic, and reversible (sufficient for the reconstruction of the original object). In the discrete case, the *Exact Euclidean Medial Axis* (MA) is also reversible and centered, but it no longer preserves topology, and it is no longer thin.

For reversible, homotopic, and centered skeletons, the MA can be combined with a homotopic thinning algorithm. There are several proposals of homotopic thinning algorithms for digital images, but some proposals are not correct [2]. One of the most robust and well defined frameworks for homotopic thinning, the critical kernels framework [3], is defined in the domain of abstract complexes, where an image must be represented in a doubled resolution.

A simple translation of the discrete MA to abstract complexes leads to undesirable thickness of the resulting skeleton. To solve this problem, Saúde et al. [4] have defined a *discrete Euclidean Medial Axis in Higher Resolution* (HMA). Such definition is a generalization of the MA definition, and it is also based on the concept of maximal balls. The combination of the HMA with the homotopic thinning based on critical kernels have resulted in satisfactory Euclidean homotopic skeletons.

The drawback of the HMA is its computational time complexity. The algorithm that computes the HMA is based on the algorithm proposed by Rémy and Thiel for the MA [5], which is not $\mathcal{O}(n)$. So, since the homotopic thinning based on critical kernels is $\mathcal{O}(n)$, the HMA is the bottleneck of the skeletonization process.

There are other definitions of Euclidean skeletons which are not based on maximal balls. Saito and Toriwaki [6] have explored the *upper envelope skeleton*. By this concept, the authors compute a set of paraboloids based on the Euclidean distance transform, and they get the centers of paraboloids in the upper envelope of all paraboloids as an Euclidean skeleton. We explain better this concept in Section 3.1.

*Corresponding author. Supported by Fapemig, Brazil.

The advantage of Saito and Toriwaki's skeleton, if compared to the MA, is computation time. The authors have proposed a fast algorithm to compute the upper envelope skeleton, and later some authors have optimized the algorithm [7]. The upper envelope skeleton can be computed in $\mathcal{O}(n)$. In the other hand, the upper envelope skeleton has a great drawback. Although the continuous upper envelope skeleton is a subset of the continuous MA, its discrete version is not a subset of the discrete MA, and it can not be used in practice.

Recently, Coeurjolly and Montanvert [8] have corrected the upper envelope skeleton for the discrete case, and they have proposed the *Reduced Discrete Euclidean Medial Axis* (RDMA). The authors prove that the RDMA is a reversible subset of the MA, and it can be computed by a $\mathcal{O}(n)$ separable algorithm.

In this paper we extend the RDMA to the higher resolution, so it can be combined with thinning algorithms on the domain of abstract complexes, and we define the *Higher-resolution Reduced Euclidean Medial Axis* (HRDMA). The HRDMA is reversible, and it can be computed in $\mathcal{O}(n)$. It can be used in place of the HMA in most practical applications.

This paper is organized as follows. In Sections 2 and 3 we recall the basic notions about Euclidean medial axes, necessary for the comprehension of this paper. In Section 4 we present our novel contribution, the HRDMA, and we show some results. In Section 5 we conclude with a discussion about discrete Euclidean medial axes and how the HRDMA fits in the current state of the art scenarium. We thank other contributors in Section 6.

2 Exact discrete Euclidean medial axes

In this section we recall the definitions of the Exact Discrete Euclidean Medial Axis (MA) and the Exact Higher-resolution Discrete Euclidean Medial Axis (HMA), which are based on maximal balls.

We denote by $\mathbb{Z}$ the set of integers, and by $\mathbb{N}$ the set of nonnegative integers. For a set X, we denote by $\overline{\mathrm{X}}$ the complement of X. We denote by $(y-x)^2$ the squared Euclidean distance between two points $x \in \mathbb{Z}^n$ and $y \in \mathbb{Z}^n$.

The basis of the most part of MA algorithms is the Euclidean distance transform. A good survey on Euclidean distance transform algorithms is given in [9]. Let $\mathrm{X} \subset \mathbb{Z}^n$, the *squared Euclidean distance transform* of X, denoted by D^2_{X}, associates to each point $x \in \mathrm{X}$ its squared Euclidean distance to the nearest point in $\overline{\mathrm{X}}$: $D^2_{\mathrm{X}}(x) = \min\{(y-x)^2, y \in \overline{\mathrm{X}}\}$.

Fix $x \in \mathbb{Z}^n$ and $R \in \mathbb{N}$, we denote by $B(x,R)$ the *Euclidean ball centered in x with (squared) strict radius R*, where $B(x,R) = \{y \in \mathbb{Z}^n, (x-y)^2 < R\}$.

2.1 Classical discrete Euclidean medial axis

We give the definition of the discrete medial axis in terms of the notion of maximal balls.

Definition 1 (Maximal Ball)**.** *Let* $\mathrm{X} \subset \mathbb{Z}^n$*,* $x \in \mathrm{X}$*,* $R \in \mathbb{N}$*,*

A ball $B(x,R) \subseteq \mathrm{X}$ *is the* greatest inside ball for x in X *if it is the largest ball centered in x and included in* X*.*

A ball $B(x,R) \subseteq \mathrm{X}$ *is a* maximal ball for X *if it is not strictly included in any other ball included in* X*.*

Observe that $B(x, D^2_{\mathrm{X}}(x))$ is equal to the greatest inside ball for x in X. Also, any maximal ball is also a greatest inside ball. We recall the definition of the medial axis.

Definition 2 (Medial Axis)**.** *Let* $\mathrm{X} \subset \mathbb{Z}^n$*, the* medial axis of X*, denoted by MA*(X)*, is the set of the centers of all the maximal balls for* X*. In other words, let* $R \in \mathbb{N}$*, MA*$(\mathrm{X}) = \{x \in \mathrm{X}, B(x,R)$ *is maximal for* $\mathrm{X}\}$.

Although the medial axis has been studied since the sixties [1], efficient algorithms for the computation of the exact Euclidean medial axis remained undiscovered until the nineties. A very efficient algorithm for the MA has been proposed only in 2003 [5, 10], and no better algorithm has appeared since then.

2.2 Discrete Euclidean medial axis in higher resolution

Medial axes in doubled resolution are useful because they can be combined with thinning algorithms which are defined on the domain of the abstract complexes [3, 4, 11]. Remember that, since the discrete medial axis does not preserve topology, and since the skeletons resulted from homotopic thinning may not be reversible, these two techniques are usually combined, so a homotopic and reversible skeleton is produced.

The use of the classical medial axis (MA) on the domain of abstract complexes is not recomended. Saúde et. al [4, 11] show the drawbacks of such use, and they define the *Higher-resolution Euclidean Medial Axis* (HMA), which gives better results when combined to thinning algorithms on abstract complexes.

The definition of the HMA is similar to that of the MA. The HMA takes an object in $\mathbb{Z}^n$ and represents it in $[\frac{1}{2}\mathbb{Z}]^n$ by a transformation to the higher resolution. For the HMA definition, a ball in the higher resolution can be centered at any point of $[\frac{1}{2}\mathbb{Z}]^n$, but contains only points of $\mathbb{Z}^n$. Let us call such balls the H-balls.

Definition 3 (H-ball)**.** *Let* $x \in [\frac{1}{2}\mathbb{Z}]^n$*,* $R \in \mathbb{N}$*, we denote by* $B_h(x,R)$ *the* H-ball centered in x with (squared) strict radius R*, where*

$$B_h(x,R) = \{y \in \mathbb{Z}^n, (2y-2x)^2 < R\}.$$

The factor 2 in $2y$ and $2x$ assures that the distances in $[\frac{1}{2}\mathbb{Z}]^n$ are equal to distances in $\mathbb{Z}^n$.

We can also define maximal H-balls by the same terms of the maximal balls.

Definition 4 (Maximal H-ball)**.** *Let* $\mathrm{X} \subset \mathbb{Z}^n$*,* $x \in [\frac{1}{2}\mathbb{Z}]^n$*,* $R \in \mathbb{N}$*,*

A H*-ball* $B_h(x, R) \subseteq \mathrm{X}$ *is the* greatest inside H-ball for x in X *if it is the largest* H*-ball centered in* x *and included in* X.

A H*-ball* $B_h(x, R) \subseteq \mathrm{X}$ *is a* maximal H-ball for X *if it is not strictly included in any other* H*-ball included in* X.

Finally, the HMA is defined by the same terms of the MA, but based on H-balls.

Definition 5 (Higher-resolution Medial Axis)**.** *Let* $\mathrm{X} \subset \mathbb{Z}^n$*, the* Higher-resolution Medial Axis of X*, denoted by* $HMA(\mathrm{X})$*, is the set of the centers of all the maximal* H*-balls for* X*. In other words, let* $R \in \mathbb{N}$*,* $HMA(\mathrm{X}) = \{x \in [\frac{1}{2}\mathbb{Z}]^n, B_h(x, R)$ *is a maximal* H*-ball for* $\mathrm{X}\}$.

Some important points about the HMA:

- The set of maximal H-balls covers the entire original object, so the object can be reconstructed from the HMA. The HMA is reversible.
- The HMA is a generalization of the MA. The HMA takes on account a larger set of Euclidean balls, including the set of Euclidean balls considered by the MA. Such balls are illustrated in Figure 1. The black points in Figure 1 represent points in H-balls, which are all in $\mathbb{Z}^2$. The center of the H-balls are represented by the crossing point of two perpendicular axes. The ball in (a) is a H-ball centered in $\mathbb{Z}^2$, and the H-balls (b-d) are centered outside $\mathbb{Z}^2$. The HMA takes on account all the types of balls in Figure 1, while the MA considers only the type of balls represented in Figure 1(a).

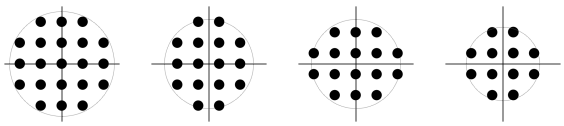

Figure 1. H-balls in $\mathbb{Z}^2$. See text.

Although the HMA definition is a simple generalization of the MA definition, the efficient algorithm that computes the MA, proposed by Rémy and Thiel [5], cannot be directly generalized for two reasons:

1. The original algorithm is based on the distance transform of the object, which is defined in $\mathbb{Z}^n$. In the higher resolution, one must compute another distance transform, in $[\frac{1}{2}\mathbb{Z}]^n$, and the usual distance transform is proven to be sufficient in 2D and 3D, but not in nD.
2. The original algorithm is based on look-up tables, and take profit of the symmetries of the Euclidean balls. The H-balls have some asymmetries which are not present in the Euclidean balls.

Despite the above difficulties, the algorithm by Rémy and Thiel was generalized in [4], but the time complexity, although similar, is greater than the time complexity of the original algorithm, and the algorithm was proved only to 2D and 3D. In a recent short communication [12], Saúde and Couprie have presented an nD version of their algorithm, which could be achieved by the use of an alternative distance transform.

In this work we show that the same alternative distance transform can be applied to the computation of another Euclidean medial axis in higher resolution, based on the upper envelope approach. Let us describe such alternative distance transform.

2.3 Distance transform to seeds

As stated before, the distance transform (DT) of an object gives the radii of the greatest inside balls for each point in the object. The algorithm by Rémy and Thiel use the DT to obtain such radii. For the higher-resolution, the values of the Euclidean DT are sufficient to determine the radii of maximal H-balls in 2D and 3D, but they are not sufficient in nD. To determine the radii of maximal H-balls in nD, a specific distance transform to seeds must be used.

The *distance transform to seeds* (DTS) is a generalization of the DT. It maps to each point of the object, its distance to the nearest point in a selected set of seeds. So, the DT is a special case of the DTS, where the set of seeds is the whole set of background points. Some DT algorithms based on distance propagation [13, 14] are already defined as DTS.

The Euclidean DTS can be computed by any Euclidean DT algorithm in two steps. Let X be the object and S be the set of seeds, do: i) compute the DT on $\overline{S}$; and ii) set to zero the points not in $\{\mathrm{X} \cap \overline{S}\}$.

We give an example of the DTS in Figure 2. The black points, with value zero, are the points of the background. The circled points are the seeds. Values greater than zero are represented on the object points, and such values are equal to the distance of each object point to the nearest seed.

For an object $\mathrm{X} \in [\frac{1}{2}\mathbb{Z}]^n$, if we choose the set $S = \overline{\mathrm{X}} \cap \mathbb{Z}^n$ as seeds, the values of the DTS from X to the seeds S are equal to the radii of the greatest inside H-balls of X in nD. The DTS illustrated in Figure 2 is exactly this specific DTS. The algorithm of the HMA works on nD if this specific DTS is used instead of the usual DT.

In Section 3 we recall the definition of a medial axis based on upper envelopes.

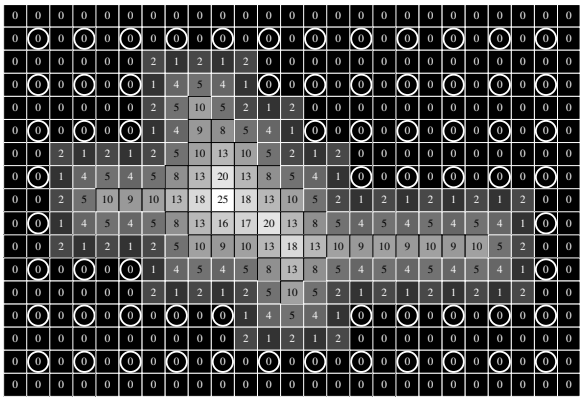

Figure 2. Distance transform to seeds.

3 Reduced discrete Euclidean medial axis

As stated in Section 2, the value of the distance transform (DT) in a point x gives the radius of the greatest inside ball for x. In fact, in digital spaces, the DT is the basis for most medial axis extraction algorithms, even the algorithms not based on the maximal balls approach. However, until the nineties, there were fast DT algorithms for other metrics (discrete distances) but not for the Euclidean metric.

In 1994, Saito and Toriwaki [6] have provided a fast (but not optimal) algorithm for the Euclidean DT. Hirata [7] was the first to provide an optimized version of such algorithm.

We explain the concept introduced by Saito and Toriwaki [6]. Consider that we want to compute the Euclidean DT of an object $\mathrm{X} \in \mathbb{Z}^n$. We take one point $x \in \overline{\mathrm{X}}$ and we compute P_x, which is an unbounded image whose values are the distances from x to every point in $\mathbb{Z}^n$. In 1D, P_x is a parabola; in 2D, P_x is a paraboloid; in nD, P_x is a hyperparaboloid. Let $S_p = \{P_y, y \in \overline{\mathrm{X}}\}$, which is the set of all hyperparaboloids centered in points $y \in \overline{\mathrm{X}}$. To find an efficient algorithm for the Euclidean DT, Saito and Toriwaki have exploited three important observations about S_p:

1. The value of the DT in a point $w \in \mathrm{X}$ is the minimum value given (to the point w) by all hyperparaboloids in S_p. If we take all $w \in \mathrm{X}$, the DT is the *lower envelope* of S_p.

2. A hyperparaboloid can be constructed by the following separable algorithm: i) construct a parabola; ii) from each point of the parabola, construct a parabola in a higher dimension; iii) do so for all the dimensions. Saito and Toriwaki prove that the lower envelope of S_p can also be computed by a separable algorithm, and the challenge is to find an efficient algorithm to compute the lower envelope in 1D.

3. Finally, in 1D, there are fast algorithms to compute the lower envelope of the parabolas. Saito and Toriwaki did not propose an optimal in time computation of the 1D problem. That was the problem solved by Hirata [7]. Since 1996 the Euclidean distance transform can be computed in linear time.

We illustrate the above concept in Figure 3. Note that the values in the centers of the parabolas are not zero, which means that such parabolas have been constructed based on parabolas resulted from a previous dimension.

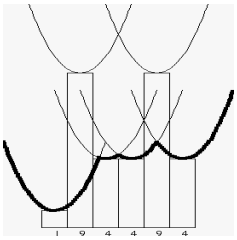

Figure 3. Lower envelope of parabolas.

In the following sections we show how this concept of lower envelope can be used to compute skeletons.

3.1 Upper envelope skeleton

Saito and Toriwaki have also proposed a fast algorithm for the reverse Euclidean distance transform [15]. The reverse transform is used to reconstruct objects from its medial axis. If we take one point x in an object X, we conclude that all points $\{y \in \mathbb{Z}^n, (x-y)^2 < D^2_{\mathrm{X}}(x)\}$ are also in the object X, so we can reconstruct them from x and $D^2_{\mathrm{X}}(x)$. Note that the set $\{y \in \mathbb{Z}^n, (x-y)^2 < D^2_{\mathrm{X}}(x)\}$ is exactly the ball $B(x, D^2_{\mathrm{X}}(x))$.

Based on the idea of the distance transform described above, let us compute P'_x, which is an unbounded image whose values are equal to $D^2_{\mathrm{X}}(x) - (x-y)^2$. P'_x is also a hyperparaboloid in nD, but with a reverted concavity if compared to the hyperparaboloid used to compute the DT. Note that $B(x, D^2_{\mathrm{X}}(x))$ is the intersection of P'_x with the hyperplane $\mathbf{0}$. Thus, the reconstruction of Euclidean balls can be performed by a reconstruction of hyperparaboloids.

The most important property proved by the authors in [15], however, is that the whole object can be reconstructed by the *upper envelope* of the set $S'_p = \{P'_x\}$, where P'_x are the hyperparaboloids with reverted concavity described above. Moreover, we are able to define a skeleton as:

Definition 6 (Upper envelope skeleton)**.** *Let* $\mathrm{X} \subset \mathbb{Z}^n$, $x \in \mathrm{X}$, $y \in \mathbb{Z}^n$, $P'_x(y) = D^2_{\mathrm{X}}(x) - (x-y)^2$, *the* upper envelope skeleton of X*, is the set of the centers of all the hyperparaboloids that compose the upper envelope of the set* $\{P'_x\}$.

The upper envelope skeleton is reversible, and it can replace the classical MA in several applications. Furthermore, Saito and Toriwaki prove that the upper envelope skeleton is a subset of the MA in the continuous space, which means that the intersection of the hyperplane **0**, and a hyperparaboloid composing the upper envelope, is a maximal ball. The converse is not true since there are maximal balls that are not the intersection of the hyperplane **0** and a hyperparaboloid composing the upper envelope.

The strong point of the upper envelope skeleton is that the computation of an upper envelope is done by the same means of the computation of a lower envelope. In consequence, the linear time Hirata's algorithm can be easily manipulated to become a linear time algorithm that computes an Euclidean medial axis. This is a great advantage over the MA, because there is not such efficient algorithm to compute the MA.

The drawback of the upper envelope skeleton is due to discretization. The discrete upper envelope skeleton, unfortunately, is not a subset of the discrete MA. The upper envelope skeleton has many additional points when compared to the MA, and it is not used in practice. This problem was solved some years later by Coeurjolly and Montanvert [8], when they proposed the *Reduced Euclidean Medial Axis* (RDMA).

3.2 RDMA

Coeurjolly and Montanvert [8] have proposed the *Reduced Euclidean Medial Axis* (RDMA), which is a discrete version of the upper envelope skeleton. The authors give an algorithmic definition to the RDMA, which is in fact a correction of the algorithm proposed by Saito and Toriwaki in [15].

The problem of the discrete implementation of the upper envelope skeleton is illustrated in Figure 4.

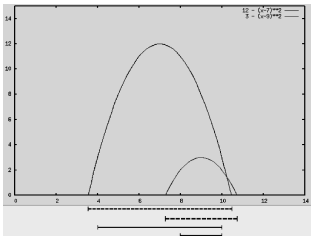

Figure 4. Continuous and discrete parabolas.

When comparing hyperparaboloids in a separable approach, the processing in the second or higher dimension may present situations like the one in Figure 4. The parabola in the left does not cover the parabola in the right. Thus, the hyperparaboloid that owns the parabola in the left does not cover the hyperparaboloid that owns the parabola in the right. In consequence, the same occurs with the projections of the parabolas on the hyperplane **0**, which are the balls. These projections are represented by the dotted segments in Figure 4. However, the set of discrete points under the left parabola contains the set of discrete points under the right parabola, which means that, in the discrete case, the left parabola covers the right parabola. This is illustrated by the straight segments represented below the dotted segments.

The authors in [8] point the problem above, and they modify the upper envelope skeleton proposed by Saito and Toriwaki by two means:

1. The 1D scans are implemented using the optimized version of the algorithm [7].

2. The algorithm does no longer test if one parabola covers another parabola. It tests if the *the set of discrete points* under one parabola contains the set of discrete points under the other parabola.

The RDMA is the skeleton resulted by this modified version of the upper envelope skeleton algorithm. This simple modification is sufficient for much better results. As discussed before, the upper envelope skeleton is a subset of the MA in the continuous case, but this property does not hold in the discrete case. The authors in [8] prove that the RDMA is a subset of the discrete MA. This property makes the RDMA more useful in practice than the original upper envelope skeleton.

Moreover, the test applied to the discrete case, as well as the test done by the original upper envelope algorithm, is performed in constant time. The 1D scan, in its optimized form, takes linear time. The algorithm for the RDMA is thus linear.

Finally, in most practical applications the RDMA can be used in place of the MA. When it is possible, the RDMA is recommended because the algorithm that computes it is faster than the algorithm that computes the MA.

In Section 4 we show a generalization of the RDMA, so it can be applied to the higher resolution, as an alternative to the HMA.

4 Higher-resolution reduced discrete Euclidean medial axis

The correction of the 1D parabola covering test proposed by Coeurjolly and Montanvert [8] can be extended to other square discrete grids. In this section we extend this concept to the doubled resolution grid, in order to define an upper envelope skeleton in a higher resolution.

The *Higher-resolution Euclidean Medial Axis* (HMA) described in Section 2.2 is defined in terms of maximal H-balls, which are Euclidean balls containing only points in $\mathbb{Z}^n$. The points in $[\frac{1}{2}\mathbb{Z}]^n$ are not part of the H-ball. By the same idea, we can extract a discretized version of the upper envelope, based on the idea of Coeurjolly and Montanvert [8], where the discrete segments which are under the continuous parabolas contain only points of $\mathbb{Z}^n$ and no points of $[\frac{1}{2}\mathbb{Z}]^n$.

One way to represent the object in the doubled resolution grid $[\frac{1}{2}\mathbb{Z}]^n$ is to expand the object by a factor of 2, so it fits exactly on the grid $\mathbb{Z}^n$. By this representation, the original points (of the normal resolution) will be placed on the points where all the coordinates are even. Every point with at least one odd coordinate is a point that appears only on the higher resolution.

If we represent our image this way, we need a simple adaptation of the algorithm in Section 3 to compare parabolas that cover discrete objects in higher resolution. This different 1D correction is illustrated in Figure 5.

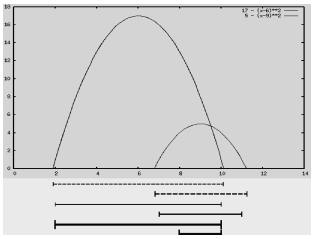

Figure 5. Continuous, discrete and higher resolution discrete parabolas.

Suppose that the situation in Figure 5 occurs while extracting the upper envelope in higher resolution. The parabola in the left does not cover the parabola in the right, as we can see by the dotted segments that represent their projection. The thin straight segments represent the discretized version of the parabolas as proposed by Coeurjolly and Montanvert [8]. The left parabola results in a segment on the interval $[2, 10]$ and center on point 6, while the right parabola results in a segment on the interval $[7, 11]$ and center on point 9. Remembering that the odd coordinates are representing points on $[\frac{1}{2}\mathbb{Z}]^n$, the center of the right segment is on $[\frac{1}{2}\mathbb{Z}]^n$. There is no problem on it, and in fact it is desirable, so we can exploit a larger number of hyperparaboloids on the image (just like the H-balls centered on $[\frac{1}{2}\mathbb{Z}]^n$). However, the points on the extremities of the right segment, those placed on the odd coordinates 7 and 11, are not necessary, since they are not in $\mathbb{Z}^n$. Thus, we can still reduce the size of the segments so we get segments that can be compared in the higher resolution. The thick straight lines represent such reduced segments. Notice that in the higher resolution the left parabola covers the right parabola.

A discretized upper envelope skeleton in higher resolution should be a subset of the HMA, so to be a real extension of the RDMA, which is a subset of the discrete MA. This property will be achieved only if the correct distance transform is used. As stated in Section 2.3, the values of the classical DT applied to the object in higher resolution are proved to be radii of greatest inside H-balls only in 2D and 3D. The distance transform to seeds presented in Section 2.3 is obligatory.

Now we are able to define an upper envelope skeleton in higher resolution. Such definition must be given in an algorithmic form, like the definition of the RDMA. The *Higher-resolution Reduced Euclidean Medial Axis* (HRDMA) is computed by the following steps:

1. The original object is transformed to the doubled resolution grid.
2. The distance transform to seeds described in Section 2.3 is computed.
3. The 1D parabola inclusion test performed by the RDMA algorithm is modified as proposed in this section, so the parabola inclusion test will work with segments as illustrated in Figure 5.
4. The above modified RDMA algorithm is applied to the distance transform to seeds computed in step 2.

In an extended version of this paper we will show if the HRDMA is a subset of the HMA. The method used by Coeurjolly and Montanvert [8] to prove that the RDMA is a subset of the MA does not seem to work directly to prove that the HRDMA is a subset of the HMA. We need to go deeper on the studies.

In the following section we show some practical results of the HRDMA in 3D objects.

4.1 Results

The main contribution of the HRDMA for practical applications is to allow programmers to tackle different kind of problems by the use of a single skeleton definition, which can be computed by a fast algorithm. The advantadges of the HRDMA are not easily detected by visual inspection, so we present the results as measurements.

We have computed the classical MA, the RDMA, the HMA and the HRDMA for ten similar but different 3D objects. The original object mean size was 3435 voxels, and its increased resolution version was 34269 voxels mean size. To estimate thinness, we have measured the ratio between the number of points in the medial axis and the number of points in the object, for all the objects in the set. The MA resulted in a mean ratio $r =$

$1230/3436 = 0.3581$. The RDMA resulted in a mean ratio $r = 873/3436 = 0.2541$. The HMA resulted in a mean ratio $r = 2532/34269 = 0.0739$. The HRDMA resulted in a mean ratio $r = 2510/34269 = 0.0732$.

In [4] the authors have measured the ratios for the MA and the HMA for a larger number of objects. We expect to do so in an extended version of this paper.

The results we have obtained are following an expected tendency: HRDMA thinner than HMA thinner than RDMA thinner than MA. We discuss the results in the following section.

5 Discussion

In this paper we have extended the definition of the RDMA [8] to the doubled resolution grid and we have defined the *Higher-resolution Reduced Discrete Euclidean Medial Axis* (HRDMA).

The main motivation for extending the RDMA is the same motivation given by Saúde et al. [4] to define the *Higher-resolution Euclidean Medial Axis* (HMA): medial axes in the doubled resolution grid can be combined with thinning algorithms which are defined in the domain of abstract complexes. We have cited a robust framework defined by Bertrand and Couprie [3]: the framework of critical kernels. It allows correct homotopic thinning algorithms to be optimal in time, and leads to unique results.

Since there is already the HMA to be combined with the critical kernels, the strongest need for the HRDMA is computation time. Compared to the available algorithms that compute the classical MA, the RDMA algorithm has two important characteritics for computation: i) linear in time ($\mathcal{O}(n)$) and ii) separable (in consequence, easy to be parallelized). We have the same advantage for HRDMA when compared to the HMA. A second need is thinness. Both the RDMA and the MA are reversible, but the RDMA has less points than the MA and produces thinner skeletons. Similarly, both the HRDMA and the HMA are reversible, but the HRDMA has less points than the HMA.

It is worth being aware that a small irregularity in the object's shape may generate important skeleton branches. The usual workaround for such undesired branches is skeleton pruning. There are several skeleton pruning algorithms in the literature and such algorithms could be applied to any of the four medial axes discussed in this paper, or to any other skeleton resulted from the combination of medial axes with homotopic thinning. Skeleton pruning is out of the scope of this paper.

Finally, let us give a more detailed comparison between the four medial axes discussed in this paper.

5.1 Comparison between Euclidean medial axes

Different medial axes can be compared in analytical and practical viewpoints. From the analytical viewpoint, notice first that all four definitions are unique, and all of them are n-dimensional. In addition:

- *Definition*. The MA and the HMA are defined in terms of maximal balls. The RDMA and the HRDMA are defined in terms of upper envelopes.
- *Thinness*. The HMA has more points than the MA but the HMA is thinner because the ratio between the number of points in the medial axis and the number of points of the object is inferior. The same situation was observed for the HRDMA, which has more points than the RDMA, but has an inferior ratio. Coeurjolly and Montanvert [8] claim that the RDMA is a subset of the MA, thus the RDMA is thinner than the MA. We have observed in tests that the HRDMA has less points than the HMA, but no property has been proven.
- *Centeredness*. Since the RDMA and the HRDMA definitions are based on upper envelopes and not on maximal balls, there is no proof that the resulting medial axis is well centered in the object according to the Euclidean distance. Only the MA and the HMA can be said centered.

In practice, the use of one definition or another will depend on the application. We describe below some observations we have had about the practical use of each of the four medial axis definitions:

- *Implementation*. About the four medial axes considered in this paper, the easier algorithms to implement are the RDMA and the HRDMA. The fastest algorithm (to our knowledge) for the MA [5] presents some difficulties in implementation. Yet more difficult to implement is its generalization that computes the HMA [4].
- *Computation time*. The computation time of the MA (by our fastest known algorithm) depends on the size of the treated object. The biggest is the object, the more complex is the computation time function. The HMA has the same behaviour. The RDMA and the HRDMA have linear time algorithms.
- *Thinness*. We have measured the ratio between the number of points in the medial axis and the number of points of the object for some objects. The ratios obtained suggest that the order of the medial axes, from the thickest to the thinner is MA, RDMA, HMA, HRDMA.

- *Centeredness*. Although not proved to be centered, in practice the results of the RDMA and the HRDMA are satisfactory.

In conclusion, after analyzing the above comparisons and the state of the art on homotopic thinning algorithms, one could note that the HRDMA is the best choice of medial axis in most of the practical cases where homotopic thinning is needed. Since the homotopic thinning algorithms are usually not so simple to implement, the simplicity of the algorithm for the HRDMA is very important. However, the most important characteristics of the HRDMA are the computation time of its algorithm and its (empirically measured) thinness.

If homotopic thinning is not needed, the RDMA can be used in place of the HRDMA. The MA or the HMA are required only if centeredness is essential.

5.2 Future works

In an extended version of this paper we will combine the HRDMA with a homotopic thinning algorithm based on critical kernels, to obtain a reversible Euclidean homotopic skeleton in linear time. We will compare the four medial axes in other real applications. We will study if the HRDMA is a subset of the HMA.

6 Acknowledgements

This work is financed by Fundação de Amparo à Pesquisa de Minas Gerais - Fapemig, grant number CEX-APQ-3457-07. The author is grateful to the collaboration of M. Couprie, from Esiee Paris, and to D. Coeurjolly, from INSA Lyon, who has provided a free C code of the RDMA.

References

[1] H. Blum. A transformation for extracting new descriptors of shape. In *Models for the Perception of Speech and Visual Form*. MIT Press, 1967.

[2] M. Couprie. Note on fifteen 2d parallel thinning algorithms. Technical Report IGM 2006-01, Institut Gaspard Monge, 2006.

[3] G. Bertrand and M. Couprie. New 3d parallel thinning algorithms based on critical kernels. In A. Kuba, K. Palágyi, and L.G. Nyúl, editors, *DGCI*, LNCS. Springer Verlag, 2006.

[4] A. V. Saúde, M. Couprie, and R. A. Lotufo. Exact Euclidean medial axis in higher resolution. In A. Kuba, K. Palágyi, and L.G. Nyúl, editors, *DGCI*, volume 4245 of *LNCS*, pages 605–616. Springer Verlag, Oct 2006.

[5] E. Rémy and E. Thiel. Exact medial axis with Euclidean distance. *Image and Vision Computing*, 23(2):167–175, 2005.

[6] T. Saito and J. I. Toriwaki. New algorithms for Euclidean distance transformation of an n-dimensional digitized picture with applications. *Pattern Recognition*, 27:1551–1565, 1994.

[7] T. Hirata. A unified linear-time algorithm for computing distance maps. *Information Processing Letters*, 58(3):129–133, 1996.

[8] D. Coeurjolly and Annick Montanvert. Optimal separable algorithms to compute the reverse euclidean distance transformation and discrete medial axis in arbitrary dimension. *IEEE Trans. on PAMI*, 29(3):437 – 448, March 2007.

[9] R. Fabbri, L. F. Costa, J. C. Torelli, and O. M. Bruno. 2D Euclidean distance transform algorithms: a comparative survey. *ACM Computing Surveys*, 40:1–44, 2008.

[10] E. Rémy and E. Thiel. Look-up tables for medial axis on squared Euclidean distance transform. In *DGCI*, volume 2886 of *LNCS*, pages 224–235. Springer Verlag, 2003.

[11] M. Couprie, A. V. Saúde, and G. Bertrand. Euclidean homotopic skeleton based on critical kernels. In *SIBGRAPI*, pages 307–314. IEEE CS press, 2006.

[12] A. V. Saúde and M. Couprie. Distance transform to seeds: computation and application. In *Extended Abstracts of the International Symposium on Mathematical Morphology (ISMM2007)*, 2007.

[13] O. Cuisenaire and B. Macq. Fast euclidean distance transformation by propagation using multiple neighborhoods. *Computer Vision and Image Understanding*, 76(2):163–172, November 1999.

[14] A. X. Falcão, J. Stolfi, and R. A. Lotufo. The Image Foresting Transform: Theory, algorithms and applications. *IEEE Trans. on PAMI*, 26(1):19–29, JAN 2004.

[15] T. Saito and J. I. Toriwaki. Reverse distance transformation and skeletons based upon the Euclidean metric for n-dimensional digital pictures. *IEICE Trans. Inf. & Syst.*, E77-D(4):1005–1016, Sep 1994.